NASA Technical Memorandum 106073

Analysis of MMIC Arrays for Use in the Acts Aero Experiment

M. Zimmerman
Analex Corporation
Brook Park, Ohio

and

R. Lee, E. Rho, and Z. Zaman
Lewis Research Center
Cleveland, Ohio

March 1993

NASA

ANALYSIS OF MMIC ARRAYS FOR USE IN THE ACTS AERO EXPERIMENT

M. Zimmerman
Analex Corporation
3001 Aerospace Parkway
Brook Park, Ohio 44142

and

R.Lee, E. Rho, and A. Zaman
National Aeronautics and Space Administration
Lewis Research Center
Cleveland, Ohio 44135

The Aero Experiment is designed to demonstrate communication from an aircraft to an Earth terminal via the ACTS. This paper describes the link budget and antenna requirements for a 4.8 kbps full-duplex voice link at Ka-band frequencies. Three arrays, one transmit array developed by TI and two receive arrays developed by GE and Boeing, were analyzed. The predicted performance characteristics of these arrays are presented and discussed in the paper.

I. INTRODUCTION

The Advanced Communications Technology Satellite (ACTS) project has as one of its goals the demonstration of Ka-band communications technology. One of the planned demonstrations is the Aero Experiment. In this experiment, an airplane will communicate with the ground via the ACTS satellite. The uplink from the airplane to the satellite will be at 29.5 GHz and the downlink from the satellite to the airplane will be at 19.7 GHz. Three arrays will be used for this experiment. Texas Instruments (TI) is building the transmit array (under NASA Lewis Research Center Contract No. NAS3-25718) and General Electric (GE) and Boeing are each building a separate receive array as subtasks to existing Rome Labs/Milstar development contracts. To predict the outcome of this experiment, an analysis has been conducted to study the array characteristics. In this report, results for the directivity, phase quantization errors, pointing accuracy and scan loss of these arrays are presented and discussed.

II. LINK ANALYSIS

In order for communication to take place, the link budget must be met by all three antennas. Table 1a and 1b present the link budget for a full-duplex voice link of 4.8 kbps BPSK with BER=10^{-3} connecting the aircraft to the ACTS ground station via the ACTS west scan sector beams. As indicated, an EIRP of 22.5 dBW for the return link and a G/T of -24.5 dB/K for the forward link is required to close the link with about 3.0 dB gain margin. It should be notes that in this report, array performance is shown in terms of directive gain. For transmit arrays, EIRP is the product of the antenna's directive gain (gain relative to an isotropic radiator emitting the same power) and the input power in Watts to the array elements. For receive antennas, the G/T (gain/temperature ratio) depends not only on the antenna's directive gain, but also on the noise temperature of the receive components, such as the phase shifters and LNA.

III. ARRAY DESCRIPTION

The geometries of the three arrays are shown in Figure 1, and their important features are summarized in Table 2. The transmit array is built from two 4x4 TI subarray modules. The TI subarray module, as shown in Fig. 1(a), has separate antenna and RF/DC circuit layers stacked in a 'tile' configuration. The aperture-coupled circular patch antenna elements are arranged in a square lattice, and are spaced 0.82 cm apart. Each patch element is connected to a 100 mW amplifier and a 4-bit phase shifter. Fig. 1(b) shows the 2x8 GE receive array in a 'brick' configuration with each card containing eight printed dipoles and their corresponding beamforming networks. The radiating elements are arranged in a triangular lattice with element spacing of 0.84 cm and lattice angular orientation of 60°. Each element is connected to its own amplifier and a 3-bit phase shifter. For comparison purpose, a 4x4 array of brick configuration with same element spacing and angular orientation has also been analyzed. At the time of writing, GE was considering building an 8x2 array with a rectangular, rather than triangular, grid lattice for cost reasons. Using a rectangular lattice rather than a triangular lattice for the 8x2 goemetry is not expected to significantly detract from the antenna performance. The Boeing array, as shown in Fig. 1(c), contains 23 elements arranged in alternating rows of 5 and 4. The elements are spaced 0.813 cm apart in a 60° triangular lattice . Each element is connected to a 4-bit phase shifter. The radiating elements are circular waveguides loaded with Rexolite ($\varepsilon_r = 2.54$) having diameter = 0.665 cm. In the analysis, the waveguides are modeled as being unloaded with diameter = 1.086 cm. Both the Boeing and GE array operate at 19.7 GHz.

IV. RESULTS AND DISCUSSIONS

The array characteristics in this report were calculated using a generalized planar array computation code, PARCOM, written by Martin Zimmermen for NASA LeRC. This program calculates the array pattern by multiplying the element pattern by the array factor. Thus, mutual coupling is not taken into account except to the extent that the element patterns used are the actual element patterns measured in an array environment. For theTI array, mutual coupling between elements is down 30 dB, so its effects can be ignored. For the other two arrays, interelement spacing is about half a wavelength so mutual coupling may have an effect. Mutual coupling can lead to a broader main beam, higher sidelobes, and array blindness at certain scan angles. In this report, characteristics such as far-field pattern shape, scan loss, phase quantization effects (pointing error and overall directive gain loss), and losses due to inaccuracies in phase shifter levels are examined. Results of the trade-off study are summarized below.

1. TI Array

The far-field pattern contour plot and cutin the ϕ=0° plane for broadside radiation for the TI 4x4 array are shown in Figures 2 and 3 respectively. In computing the radiation patterns, the element pattern is numerically modelled to match the measured element pattern provided by TI. The radiating efficiency was then adjusted to match the analytically calculated directivity with the experimental results of 5.5 dB directive gain. This lead to a radiating efficiency of 89%, which is typical for a microstrip patch. The gain of the TI 4x4 array is 17.7 dB and the EIRP is 19.3 dBW assuming 1.4 watts RF input power to the antennas. Scan loss for the 4x4 array is shown in Figure 4, which also indicates how the main beam broaden as the antenna is scanned away from boresight. Since the link budget calls for an EIRP of 22.5 dBW, the 4x4 module will

not be adequate to maintain the link for wide scans. For this reason, it was proposed that two such 4x4 modules be combined to form an 8x4 array. The 8x4 array has an array gain of 20.7 dB and an EIRP of 25.3 dBW. Note that doubling the number of elements raises the EIRP by 6 dBW because both the input power and the array gain are double. The scan loss for the 8x4 array is shown in Figure 5.

Phase quantization loss is defined as the decrease in antenna gain in a specific direction due to quantized phase shifting. In general, the amount of loss is directly related to how close the phase shifters can be set to the required phase settings for the scan. Phase quantization loss as a function of scan angle is periodic, with the period , τ, related to the element spacing , s, and the phase increment per bit, α, by the formula

$$360°\sin(\tau)\, s/\lambda = \alpha$$

Thus, for the TI array with 4-bit phase shifter (α=22.5°) and s=0.82 , the period is approximately 4.5°. The period for the same array with 3-bit phase shifter is approximately 9°. Phase quantization losses for the TI 4x4 array for the cases of 3-bit, 4-bit and 5-bit phase shifters were calculated, and these losses in the ϕ=0° plane is shown in Figure 6. As indicated, using 4-bit phase shifters decreases the directivity by less than .06 dB, and has only a small impact on the array performance. Phase quantization losses for the TI 8x4 array with 4-bit phase shifters were also calculated for ϕ=0° and ϕ=45°. Similar results were obtained and are shown in Figure 7. Phase quantization also causes pointing error in the main beam. Pointing error is a measure of the angular difference between the beam maximums with and without phase quantization. Figure 8 shows the pointing error for the TI 4x4 array module caused by phase quantization. It should be noted that beam squinting is common for arrays with medium or high gain element and this must be taken into consideration. Also, high pointing error does not automatically imply high quantization loss. If the pattern roll-off is low (i.e. broad main beam), then the phase quantization loss due to pointing error can be quite small.

Random phase errors in phase shifters often generate losses in phased arrays. This phase error is a result of inexactitudes in the manufacturing process, and is also affected by temperature and other time-dependent mechanisms. The random error losses can be modelled by a random variable that is assumed to be normally distributed. For the phase shifters used in the TI 4x4 array, the phase error has been experimentally established to have an RMS value of 7°. Using sample size of 15 (i.e. 15 runs for each scan angle), the random error losses versus scan angles for the TI 4x4 array were calculated and are shown in Figure 9. For each scan angle, the mean RMS loss is shown along with the upper and lower bounds for the 95% confidence interval. Statistically, there is a 95% probability that the true mean of the distribution is inside the confidence interval.

2. GE Array

The element patterns are modelled by a $(\cos\theta)^q$ function with q_e=0.4 and q_h=0.1. This pattern, having a 3 dB beamwidth of 130° in the E-plane and only about 2 dB rolloff in the H-plane for observation angles near ±90°, matches very well with the experimental data provided by GE. For the Aero Experiment, only 16 elements are needed to meet the link requirement. Two possible configurations; an 8x2 array and a 4x4 array, were studied. The 8x2 array, though asymmetrical, is easier and cheaper to fabricate so this tradeoff study will help GE to decide which array configuration to use. The far-field patterns for the two configurations are shown in Figures 10-12. As expected, the 8x2 array has a narrow beam in the ϕ=0° plane and a broad beam in the

ϕ=90° plane. The 3 dB beamwidth is equal to 11.5° in the ϕ=0°plane and 52° in the ϕ=90° plane. Scan losses for the two arrays are shown in Figures 13 and 14. As indicated, scan loss for the 4x4 array in the ϕ=0° plane is approximately the same as that for the 8x2 array, but is better by at least 1 dB in any other plane cuts, particularly in the ϕ=90° plane.

For the GE 8x2 array with 3-bit phase shifter (α=45°)and element spacing s=0.84 cm (0.56 λ), the period is approximately 13°. Phase quantization losses for this array with 3, 4 or 5-bit phase shifters are shown in Figure 15. For the 3-bit phase shifter case, the maximum decrease in directivity is about 0.4 dB. Figure 16 shows the pointing error for the same array in the ϕ =0° plane. Since the array is only two elements wide in the ϕ =90° plane, the pointing error can be quite high (>5°) in this plane. However, because the pattern is very broad (half-power beamwidth = 52°), the loss associated with the pointing error is not severe (less than 0.5 dB). Phase quantization loss and phase pointing error for the GE 4x4 array are shown in Figures 17 and 18 respectively. As expected, the pointing error in the ϕ=90° plane is significantly improved (less than 2°), but the quantization losses are slightly worse in both the ϕ=0° and ϕ=90° planes. The minimum phase quantization losses for the GE 8x2 and 4x4 arrays are shown in Figure 19.

The RMS error loss was calculated based on GE's estimate of 16° RMS phase error per phase shifter and 1.7 dB amplitude error per amplifier. Results are shown in Figure 20 for the GE 8x2 array with 3-bit phase shifters and sample size of 15. Because of the small sample size used, the total mean RMS loss at boresight is a much higher -0.70 dB compared to GE's figure of 0.35 dB for phase RMS loss and -0.16 dB for amplitude RMS loss. Several independent sample runs were performed separately for the phase and amplitude measurements and these all indicate a total loss at boresight of about 0.5 dB.

3. Boeing Array

The element pattern as shown in Figure 21 is determined by physical optics. The directivity for each element is 7.14 dB which yields an array gain of 19.30 dB. The Boeing array has a higher boresight directivity than the GE array. The contour plot for boresight scan is shown in Figure 23 and the boresight radiation patterns in both principal planes are shown in Fig. 22. Scan loss, including the losses due to a 4-bit phase shifter, is shown in Figure 24. Scan loss tends to be higher for an array with a more directive element pattern and the Boeing array does in fact have higher scan losses than the TI or GE arrays.

The quantization loss using optimal pointing is shown in Fig. 25. Phase quantization loss for the Boeing array is very low overall, indicating that there is no need to consider the use of 5-bit phase shifters.

V. CONCLUSION

The purpose of this study is to collect in one document information about the capabilities of the three arrays for use in the Aero Experiment. Array characteristics including scan loss, phase quantization loss, pointing and RMS error losses were analyzed. Also included in the paper are results of the link analysis of a full-duplex voice at 4.8 kbps. This study confirms that both the TI transmit array, and the GE and Boeing receive arrays meet the link budget requirements with about 3.0 dB gain margin.

Table 1a. Forward Link Analyis

(LET - ACTS - AIRCRAFT)

UPLINK (LET to ACTS)			DOWNLINK (ACTS to AIRCRAFT)		
Frequency	30.0	GHz	Frequency	20.0	GHz
LET EIRP, spec	65.0	dBW	EIRP, spec	62.7	dBW
			SIGNAL EIRP	60.7	dBW
Pointing loss	0.5	dB			
Propagation Loss	213.69	dB	Propagation Loss	210.0	dB
Range	385,000	KM	Range	378,950	KM
Atmospheric Loss	0.36	dB	Atmospheric Loss	0.5	dB
Rain Loss	0.0	dB	Rain Loss	0.0	dB
CLEVLAND G/T, sp	18.70	dB/K	AIRCRAFT G/T	-24.5	dB/K
Pol mismatch	0.3	dB	Pol mismatch	3.0	dB
C/No, up	97.4	dB-Hz	C/No, down	51.3	dB-Hz
SNR, up(BW=1GHz)	7.4	dB	C/No, achieved	51.3	dB-Hz
Limiter suppression	5.0	dB			
			C/No, required	44.8	dB-Hz
			Modem & Phase Nois	2.5	dB
QPSK or BPSK, (R=4.8 kbps, BER=1)			Fade Allowance	1	dB
			LINK MARGIN	3.0	dB

Table 1b. Return Link Analysis

(AIRCRAFT - ACTS - LET)

UPLINK (AIRCRAFT to ACTS)			DOWNLINK (ACTS to LET)		
Frequency	30.0	GHz	Frequency	20.0	GHz
AIRCRAFT EIRP (T	22.5	dBW	CLEVELAND EIRP, sp	62.7	dBW
			SIGNAL EIRP	24.5	dBW
Propagation loss	213.56	dB	Propagation loss	210.0	dB
Range	378,950	KM	Range	380,000	KM
Atmospheric loss	0.3	dB	Atmospheric Loss	0.5	dB
Rain loss	0.0	dB	Rain Loss	10.0	dB
G/T, spec	18.7	dB/K	LET G/T, spec	28.5	dB/K
Pol mismatch	3.0	dB	Pol mismatch	0.5	dB
C/No, up	52.9	dB-Hz	C/No, down	60.5	dB-Hz
SNR, up(BW=1GHz)	-37.0	dB	C/No, achieved	51.3	dB-Hz
Limiter suppression	1.1	dB			
			C/No, required	44.8	dB-Hz
QPSK or BPSK (R=4.8 kbps BER=1)			Modem & Phase Noise	2.5	dB
			Fade Allowance	1.0	dB
			LINK MARGIN	2.9	dB

Table 2. MMIC array characteristics

Contractor	Texas Instruments	General Electric	Boeing
Type	Transmit	Receive	Receive
Frequency (GHz)	29.3	19.7	19.7
No. of Elements	32	16	23
Array configuration	Tile	Brick	Brick
Element configuration	8x4 - square grid	8x2 - triangular grid	square area - tri. grid
Element spacing (cm)	0.82 (0.80 λ)	0.84 (0.55 λ)	0.81 (0.53 λ)
Radiating elements	Aperture coupled circular patch	Printed circuit dipole	Dielectrically loaded circular waveguide
Polarization	Linear	Linear	Linear
Phase shifter bits	4	3	4
Scanning range without grating lobes	±30°	±60°	±60°
Target EIRP (dBW)*	21	N/A	N/A
Target G/T (dB/degK)*	N/A	-15	-20

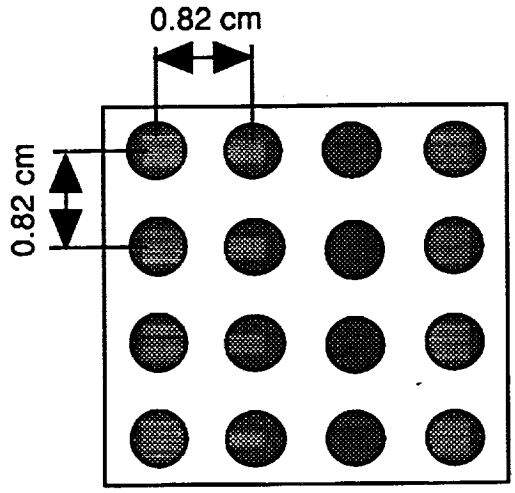

(a)

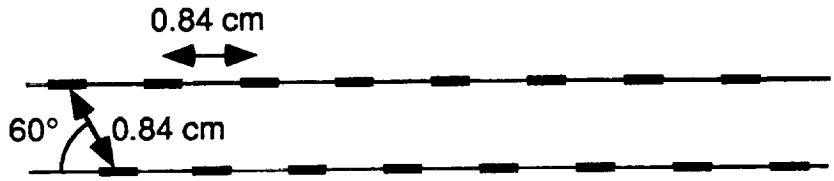

(b)

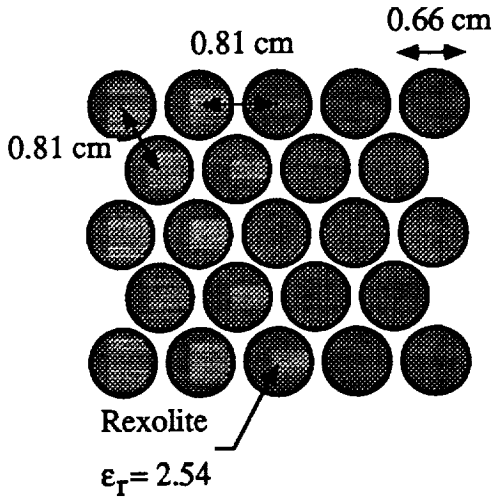

(c)

Figure 1. Array configurations: (a) Ti 4x4 array, (b) GE 8x2 array and (c) Boeing 23-element array

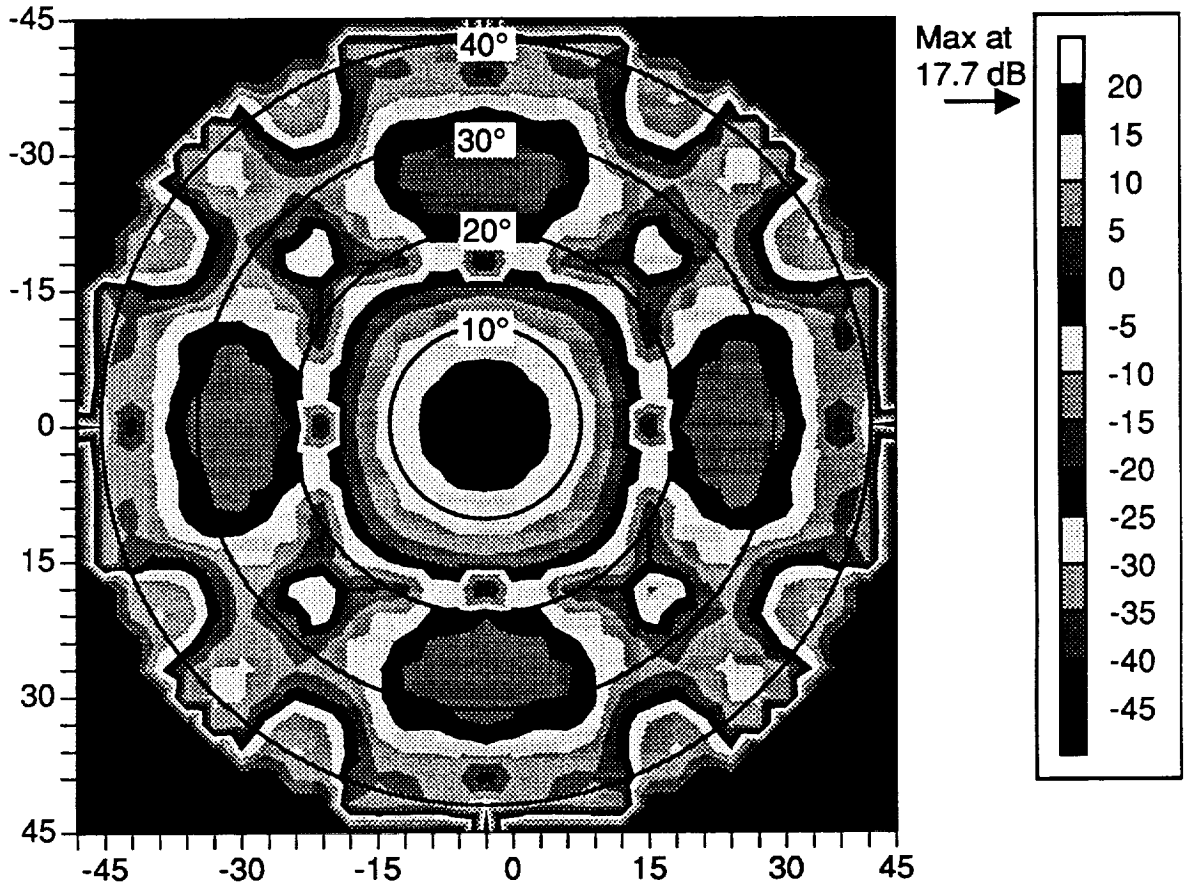

Figure 2. Far-field pattern contour plot of TI array for broadside scan and observation angles out to theta = 45°.

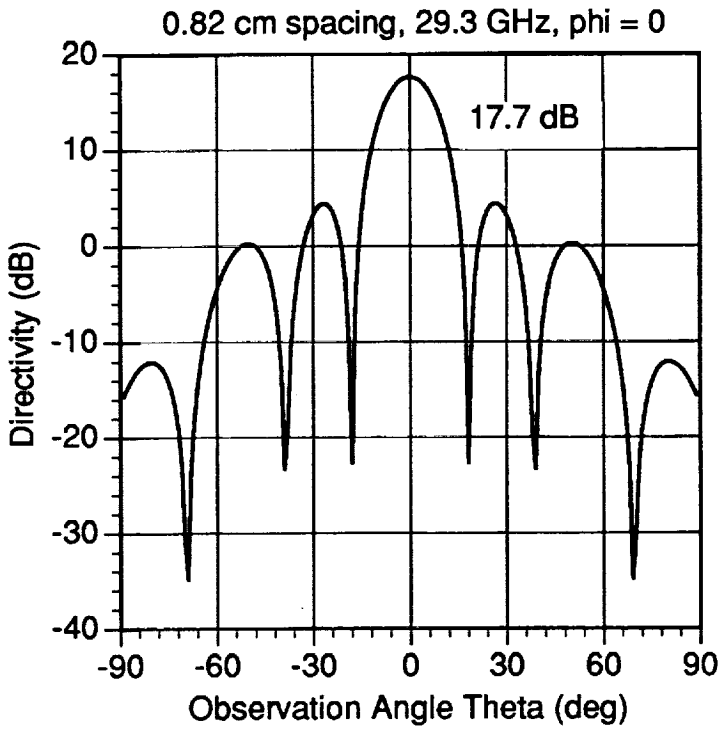

Figure 3. Pattern cut for TI 4x4 array at broadside (phi = 0°). The phi = 90° cut is similar.

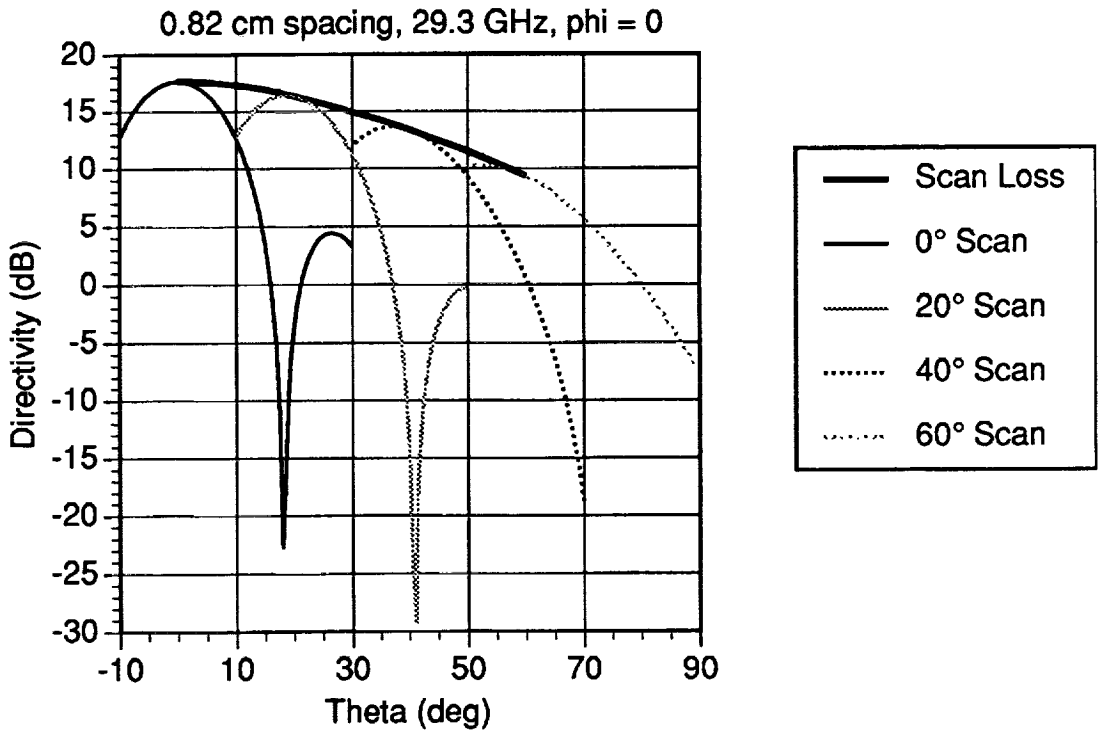

Figure 4. Scan loss for TI 4x4 array with far-field patterns at various scan angles.

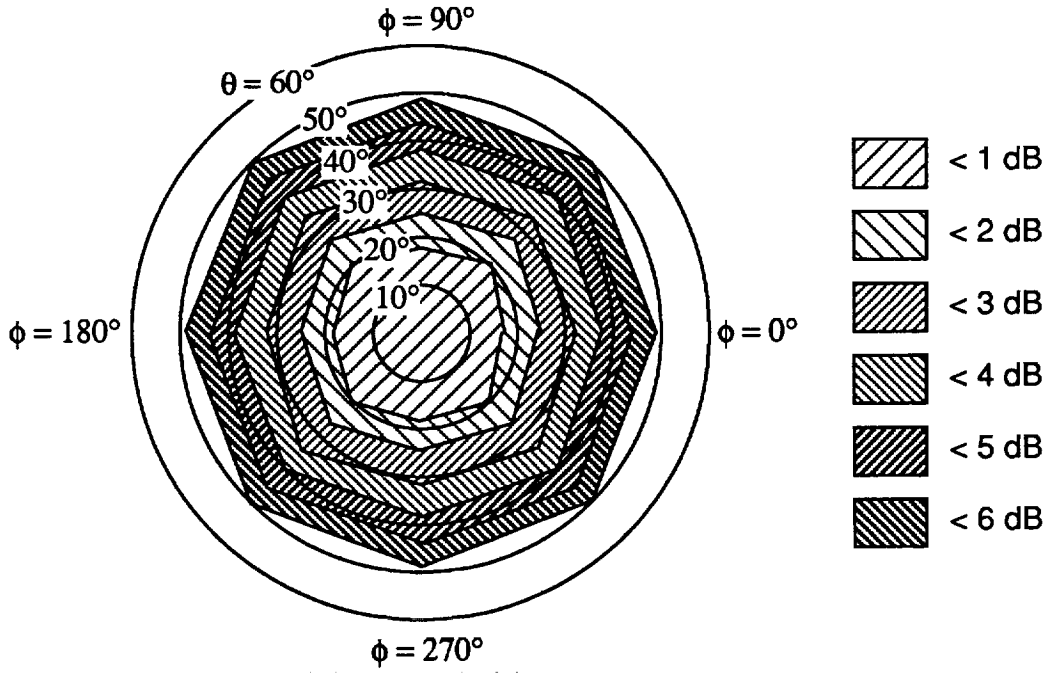

Figure 5. Scan loss for the TI 8x4 array.

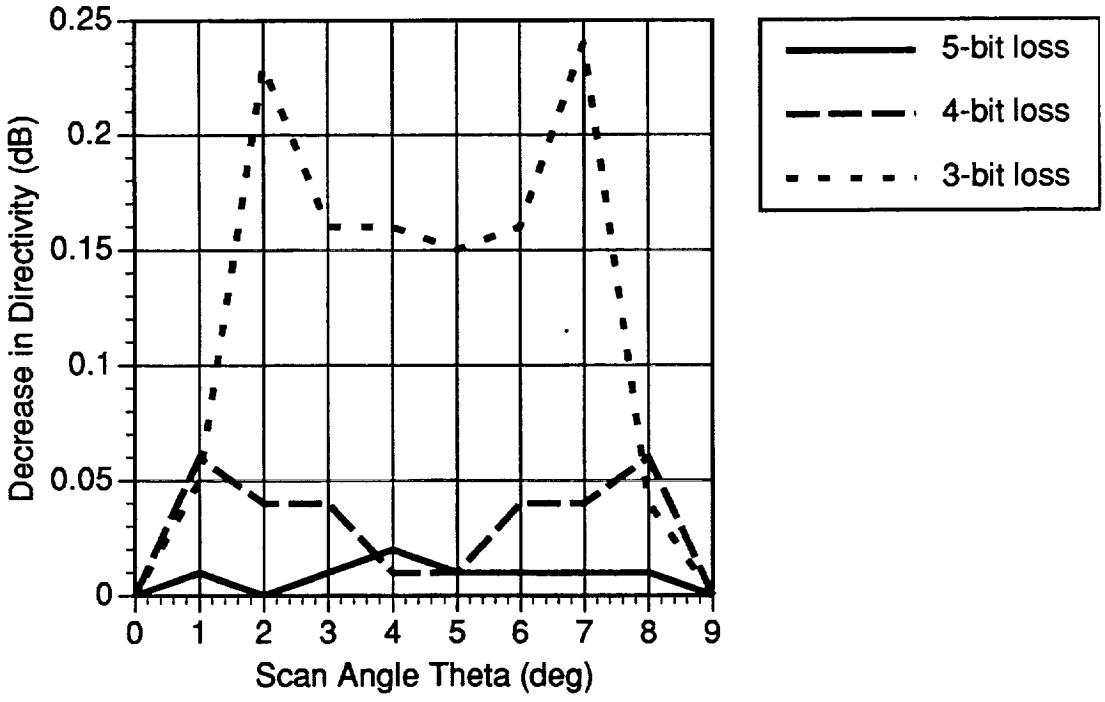

Figure 6. Phase quantization loss for the TI 4x4 array (phi = 0° plane).

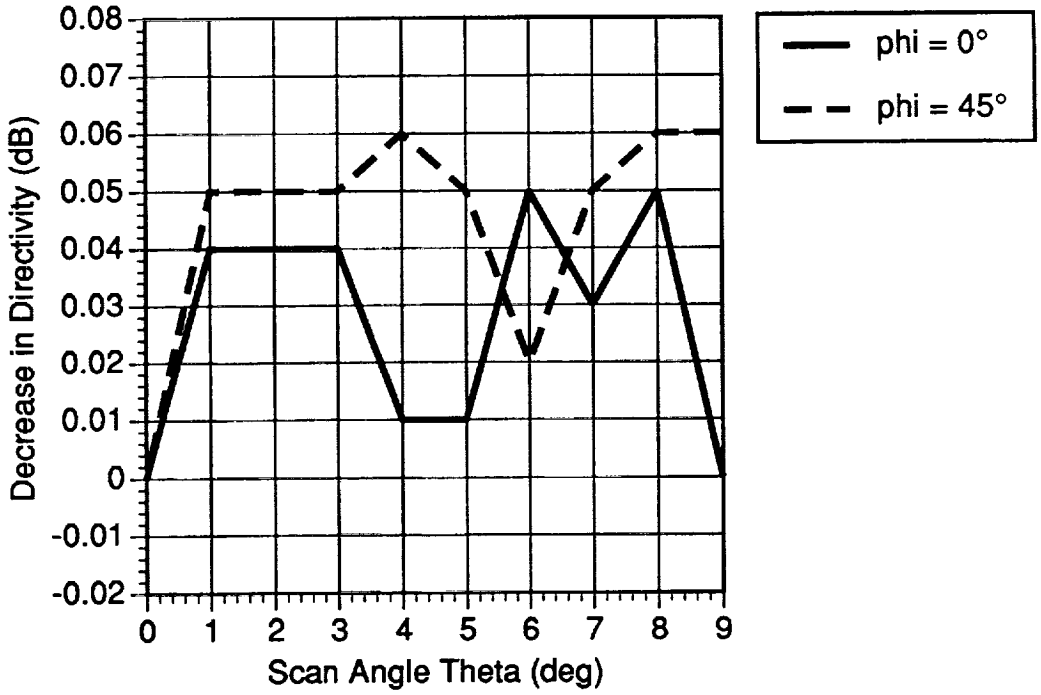

Figure 7. Minimized phase quantization loss for the TI 8x4 array using 4-bit phase shifters.

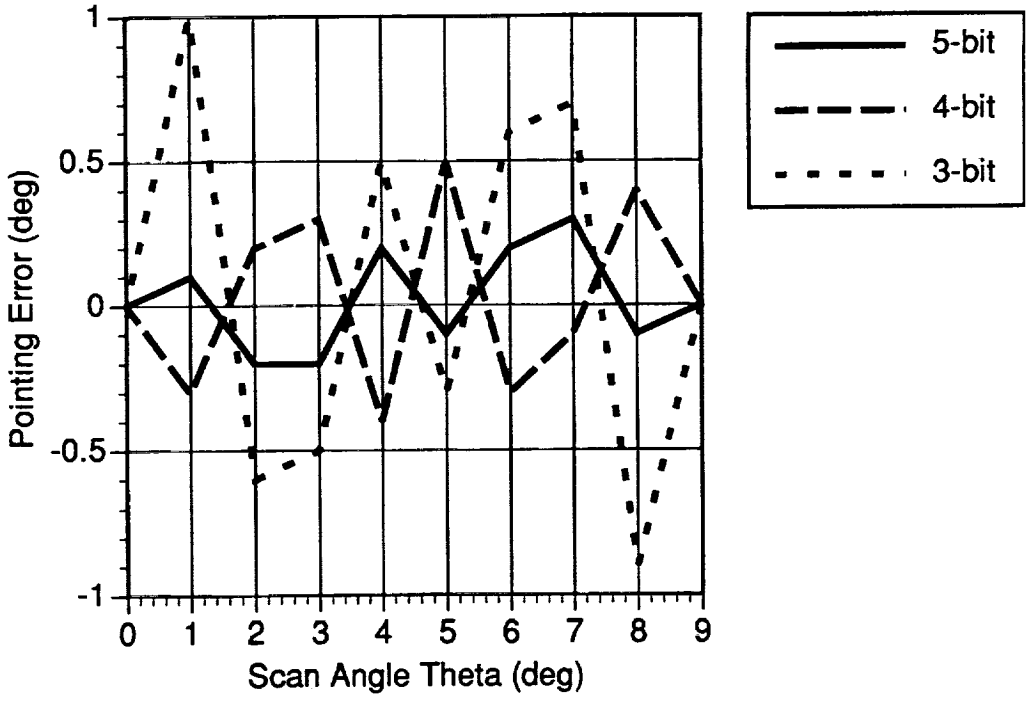

Figure 8. Phase quantization pointing error for the TI 4x4 array (phi = 0° plane).

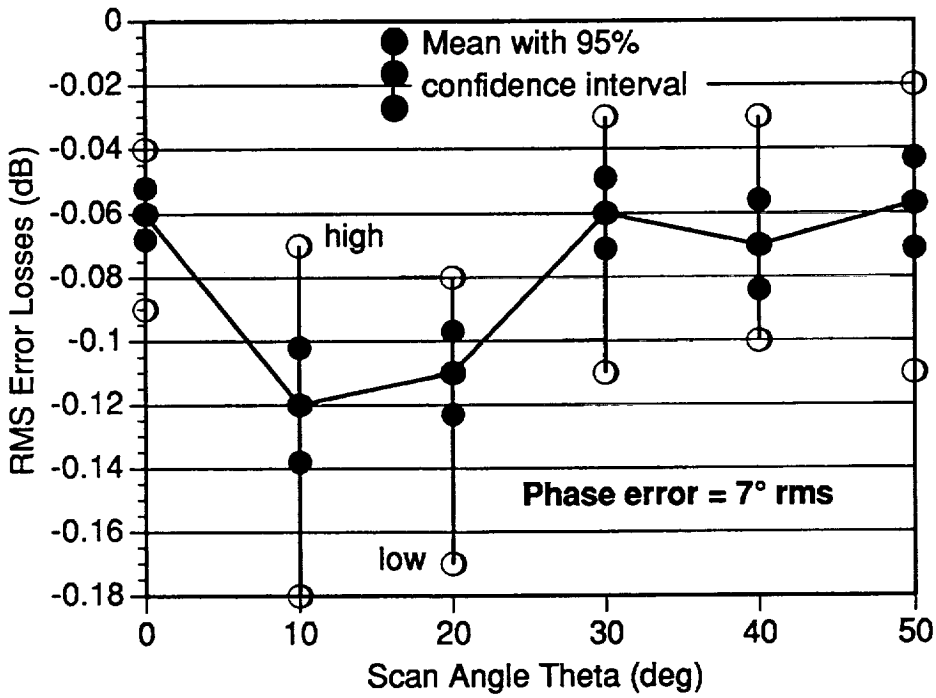

Figure 9. Random error losses for TI 8x4 array with 4-bit phase shifters.

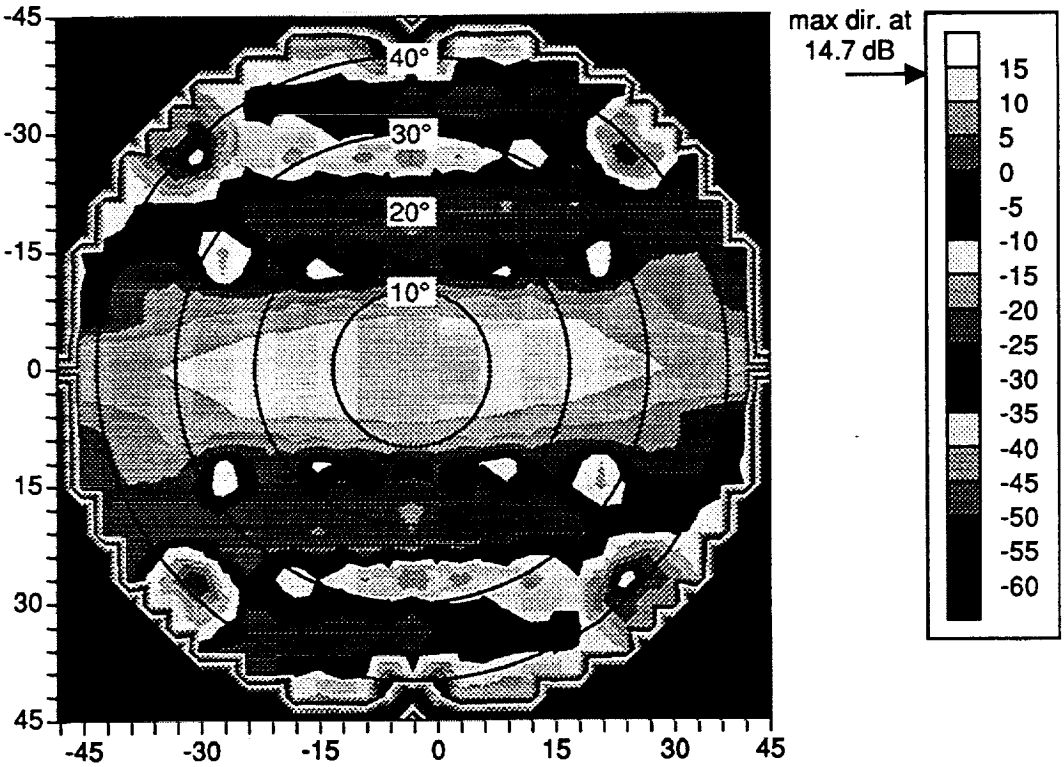

(a)

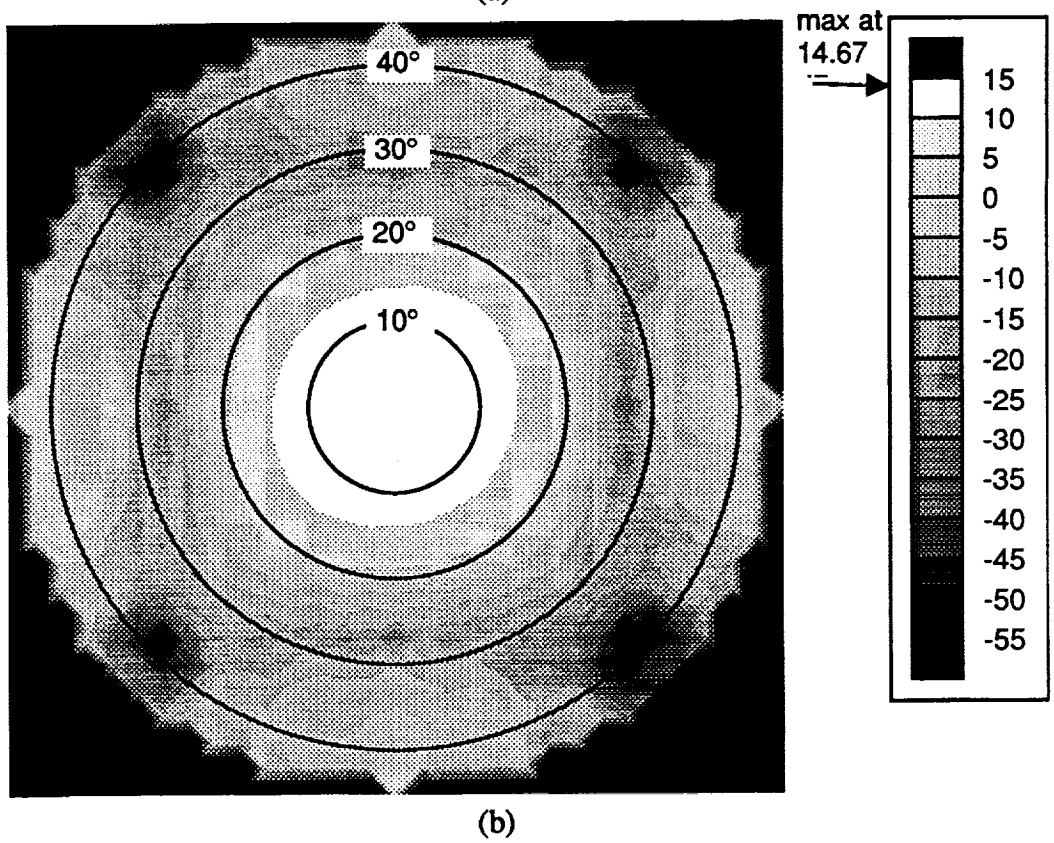

(b)

Figure 10. Contour plot of broadside far-field patterns out to $\theta = 45°$ for: (a) GE 8x2 and (b) GE 4x4 arrays.

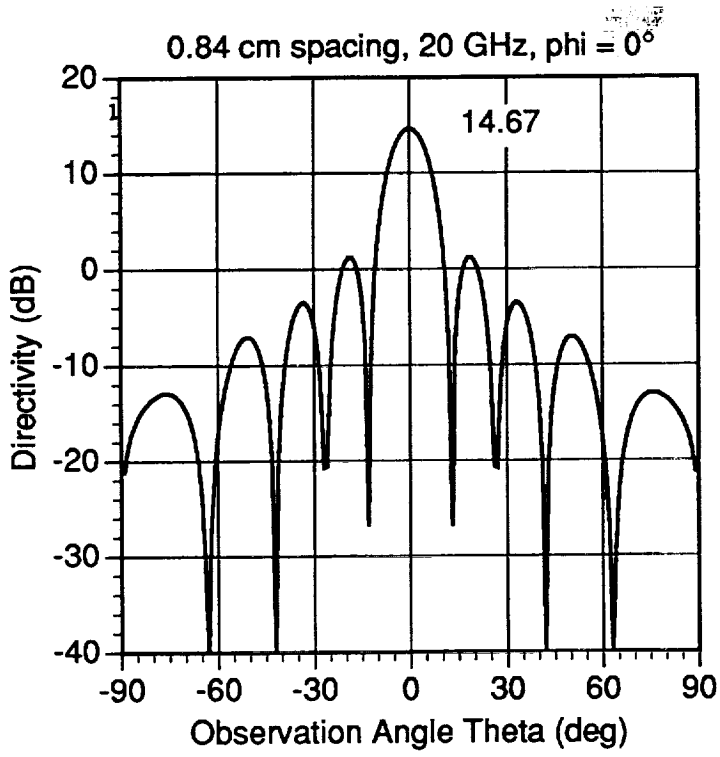

Figure 11a. Broadside far-field pattern of GE 8x2 array for phi = 0° plane.

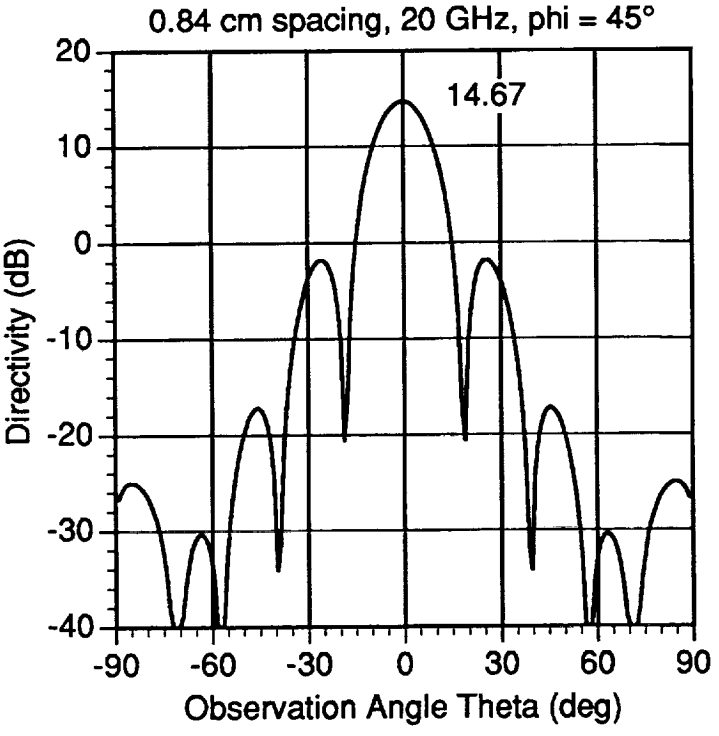

Figure 11b. Broadside far-field pattern of GE 8x2 array for phi = 45° plane.

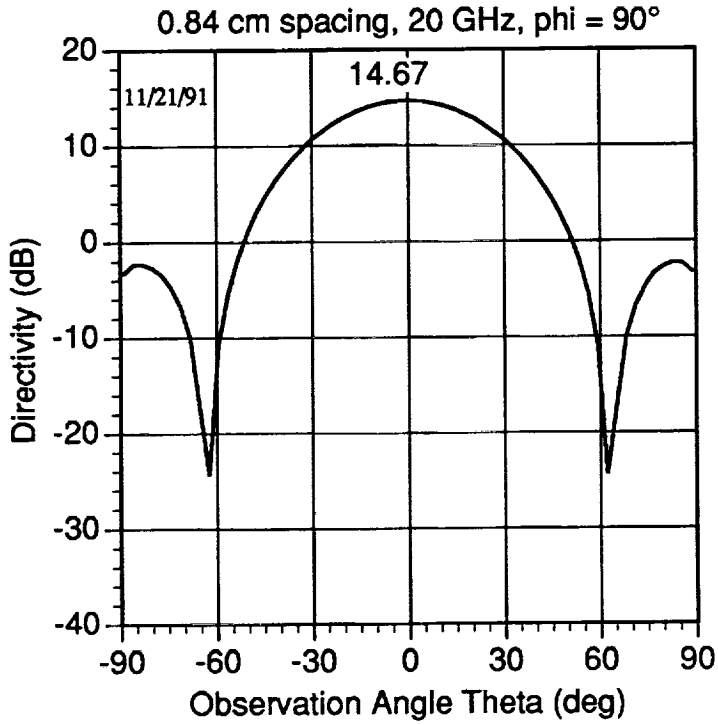

Figure 11c. Broadside far-field pattern of GE 8x2 array for phi = 90° plane.

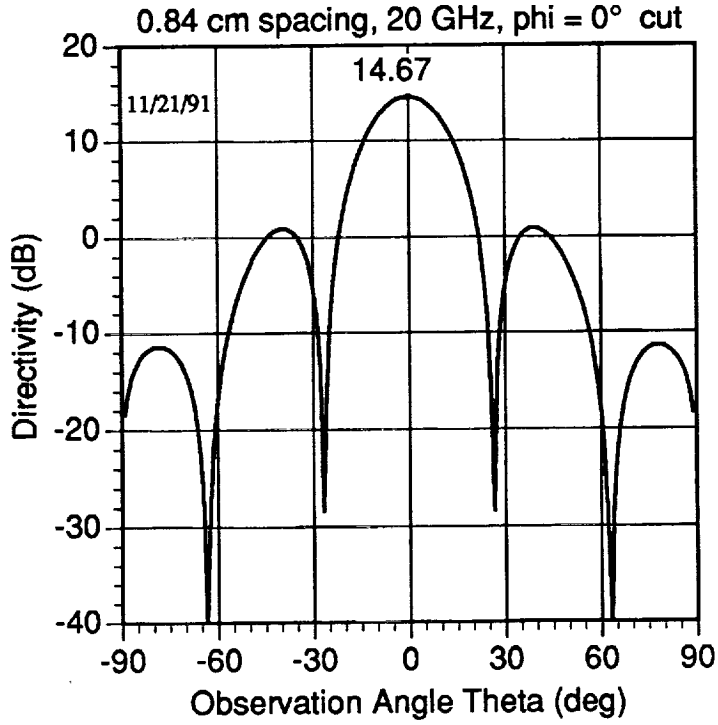

Figure 12a. Broadside far-field pattern of GE 4x4 array for phi = 0° plane.

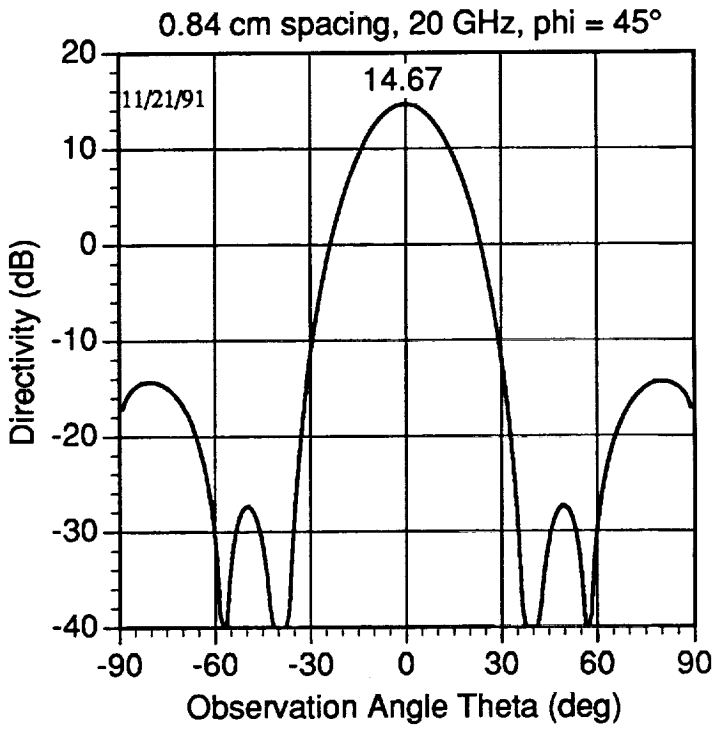

Figure 12b. Broadside far-field pattern of GE 4x4 array for phi = 45° plane.

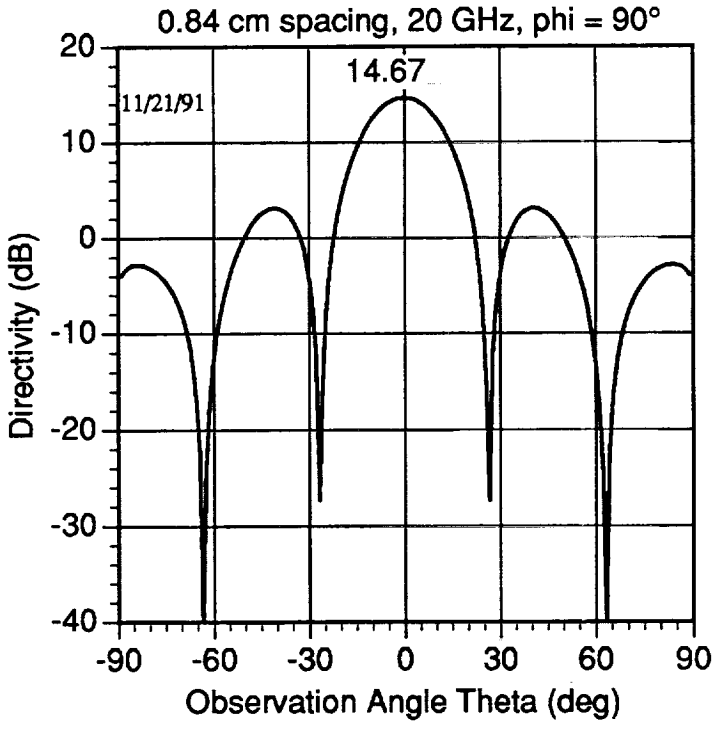

Figure 12c. Broadside far-field pattern of GE 4x4 array for phi = 90° plane.

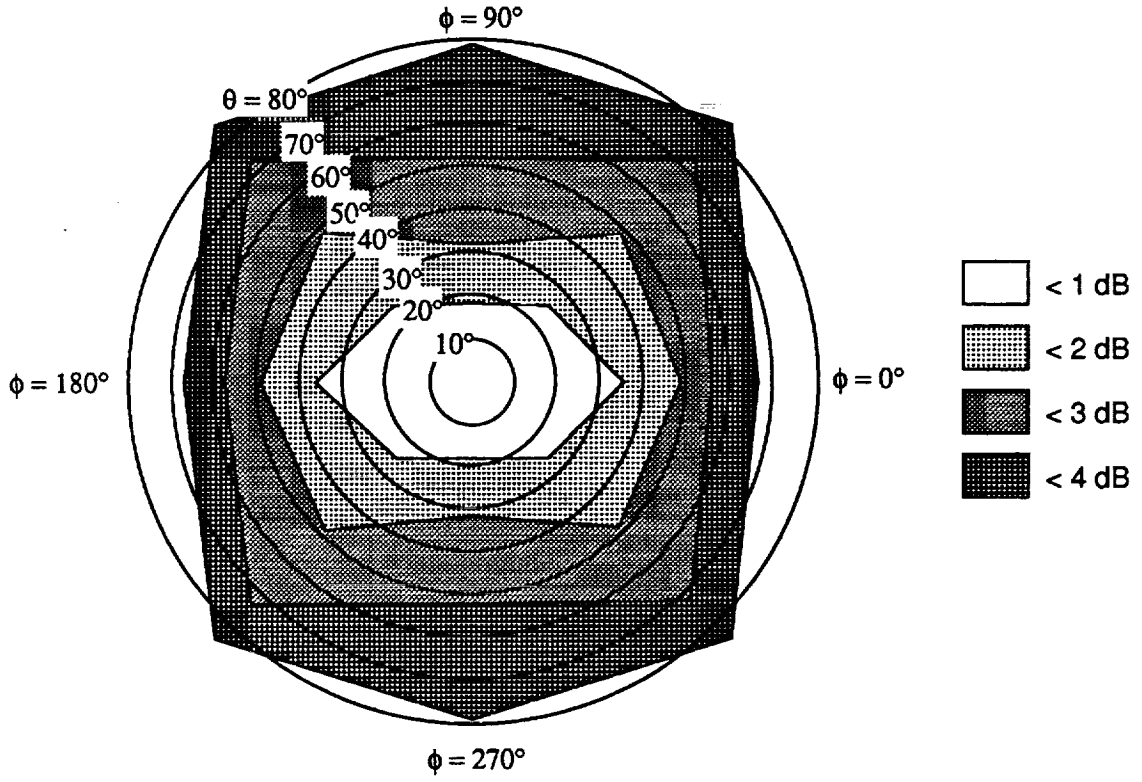

Figure 13. Scan loss for the GE 8x2 configuration.

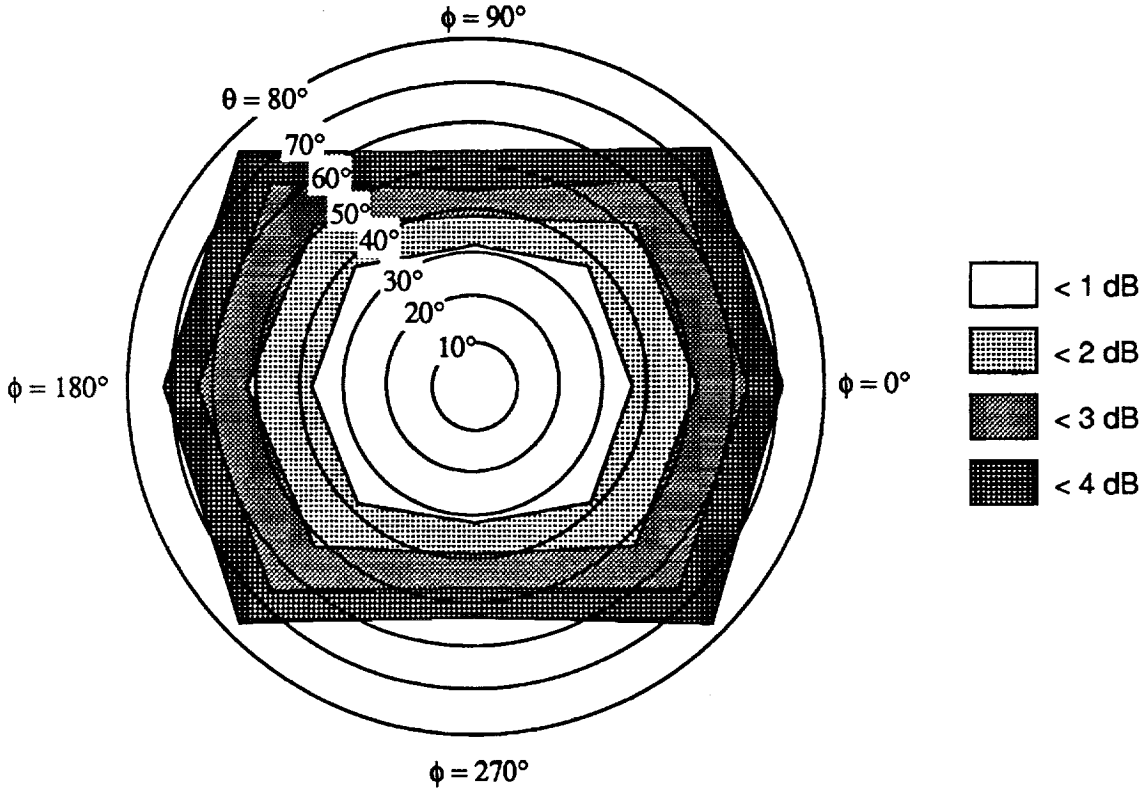

Figure 14. Scan loss for the GE 4x4 configuration.

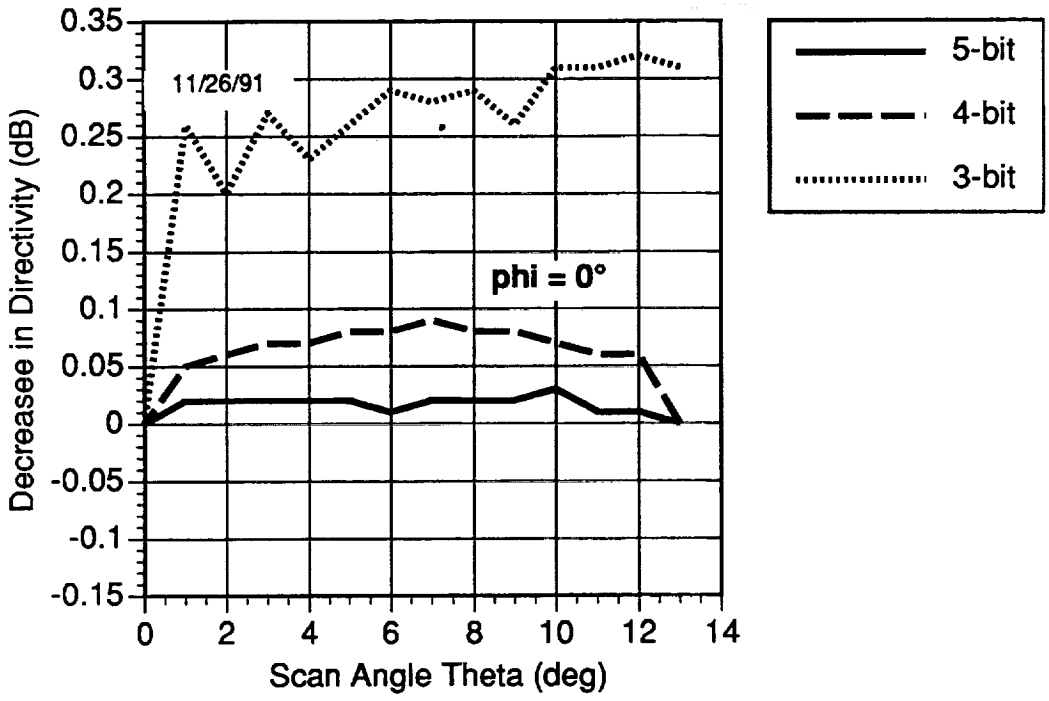

(a)

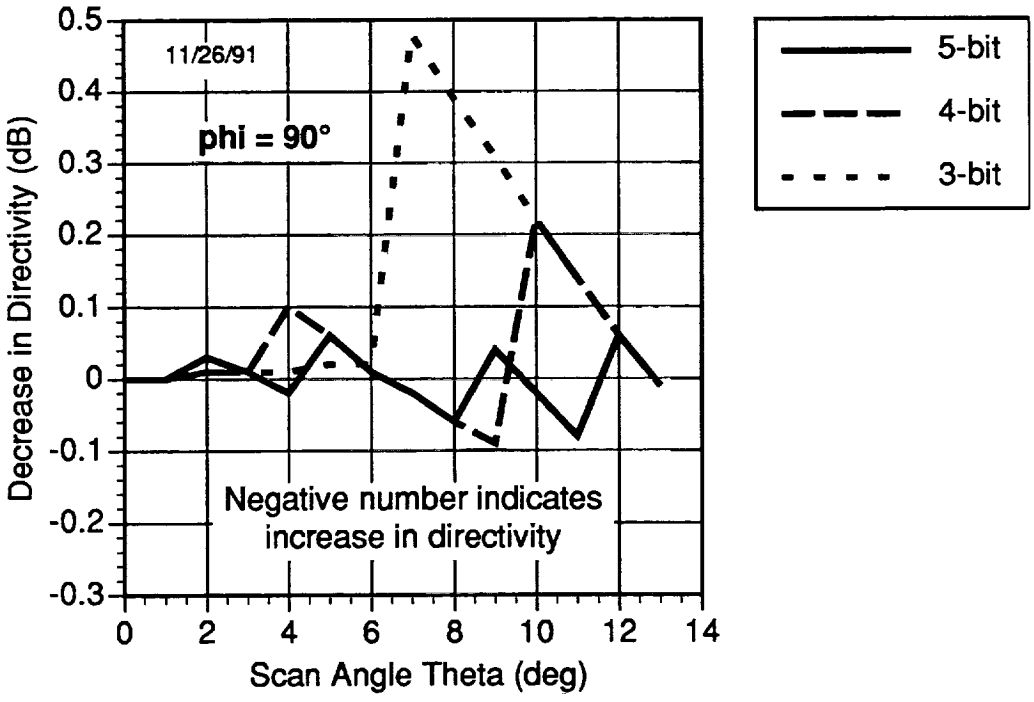

(b)

Figure 15. Phase quantization loss for GE 8x2 array for: (a) phi = 0° plane and (b) phi = 90° plane.

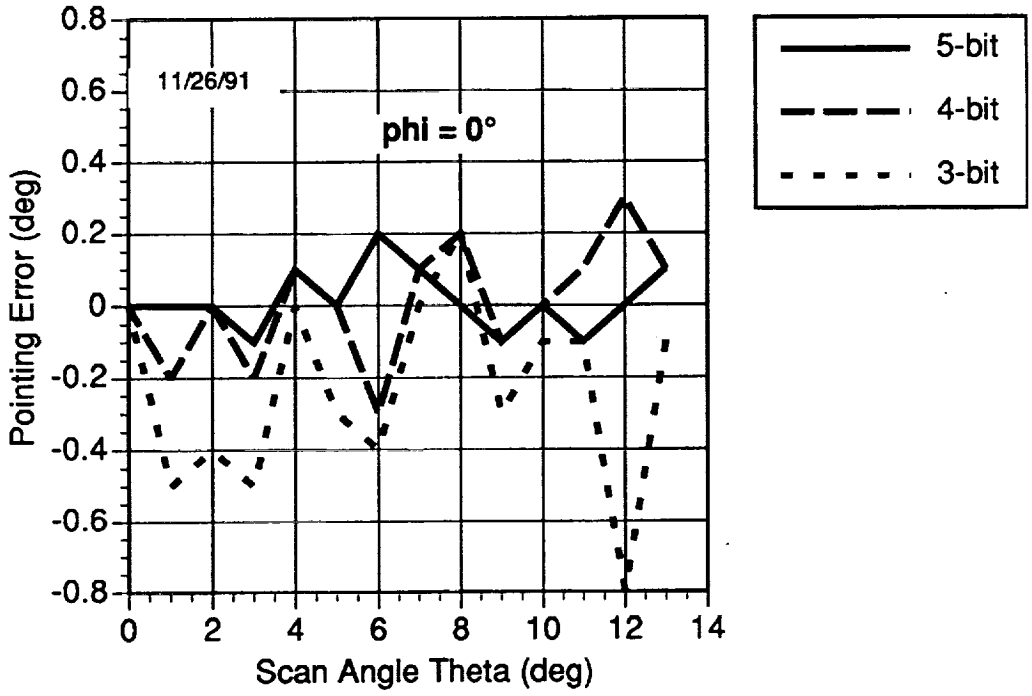

(a)

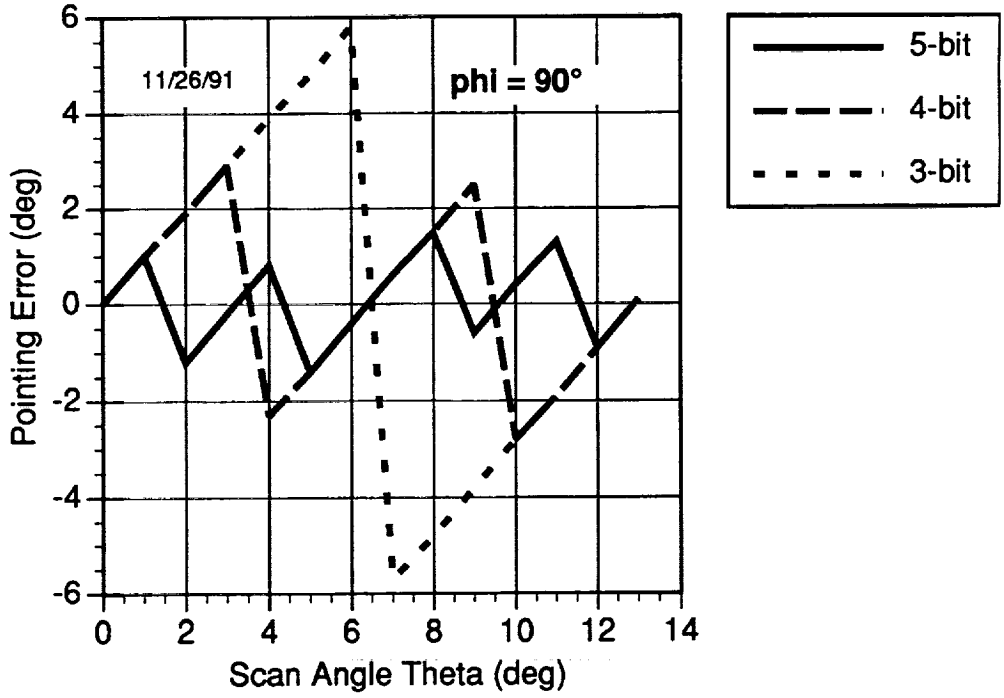

(b)

Figure 16. Phase pointing error for GE 8x2 array for: (a) phi = 0° plane and (b) phi = 90° plane.

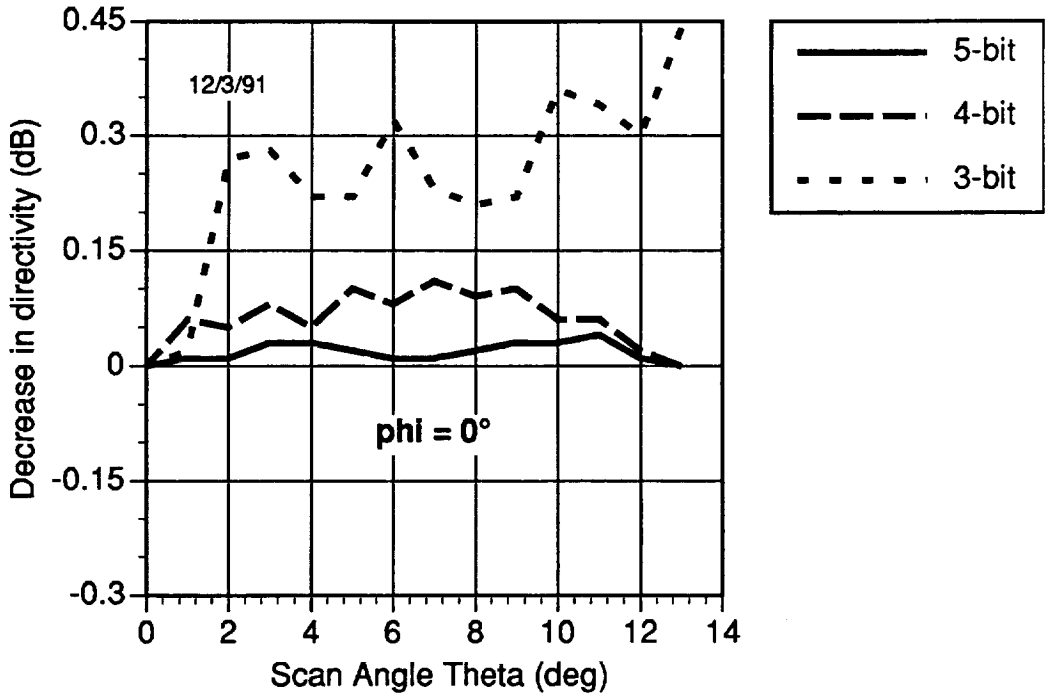

(a)

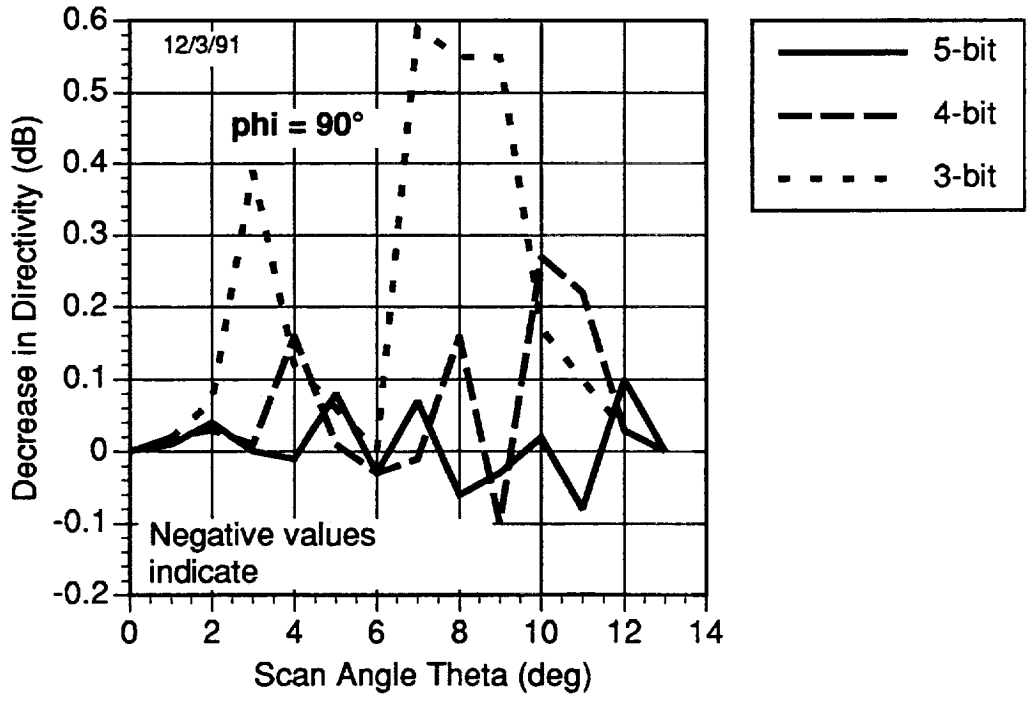

(b)

Figure 17. Phase quantization error for Ge 4x4 array for: (a) phi = 0° plane and (b) phi = 90° plane.

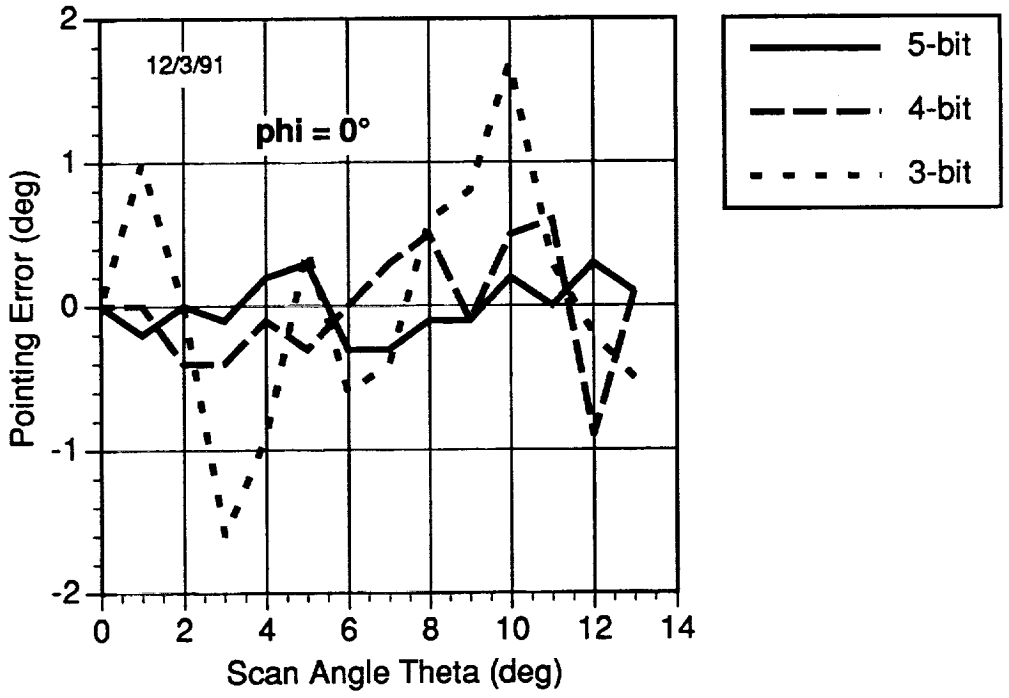

(a)

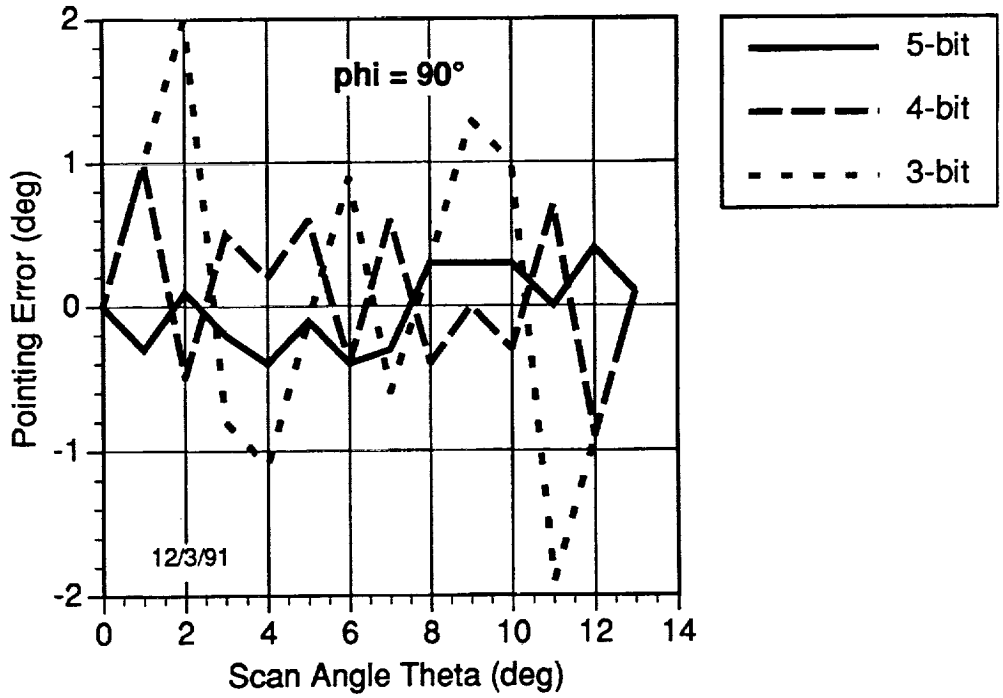

(b)

Figure 18. Phase pointing error for Ge 4x4 array for: (a) phi = 0° plane and (b) phi = 90° plane.

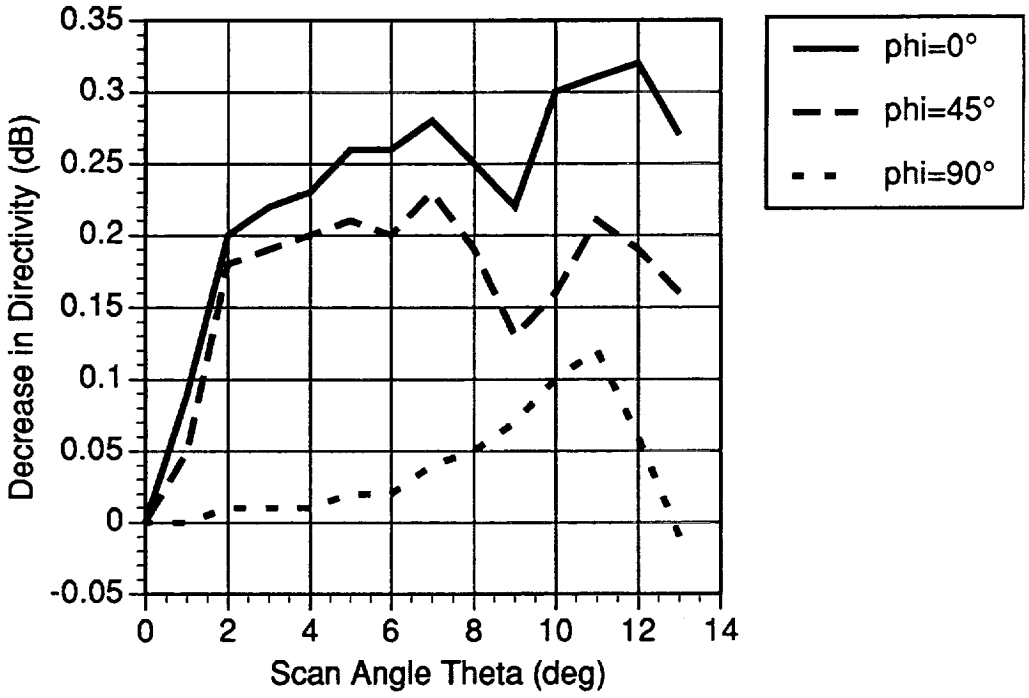

(a)

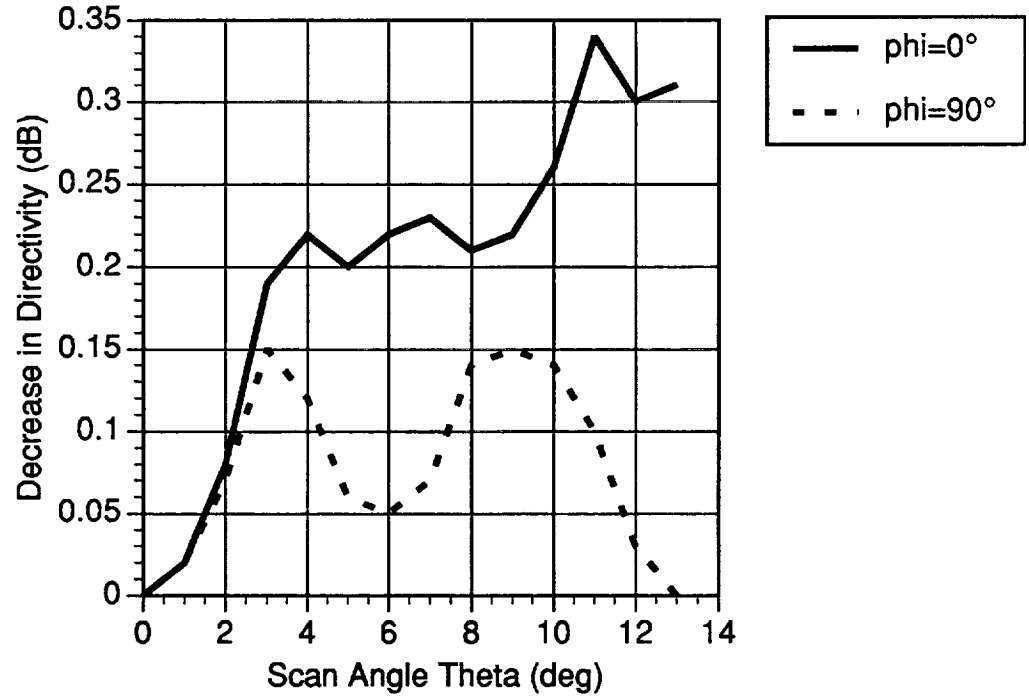

(b)

Figure 19. Minimized phase quantization loss for the: (a) GE 8x2 array and (b) GE 4x4 array.

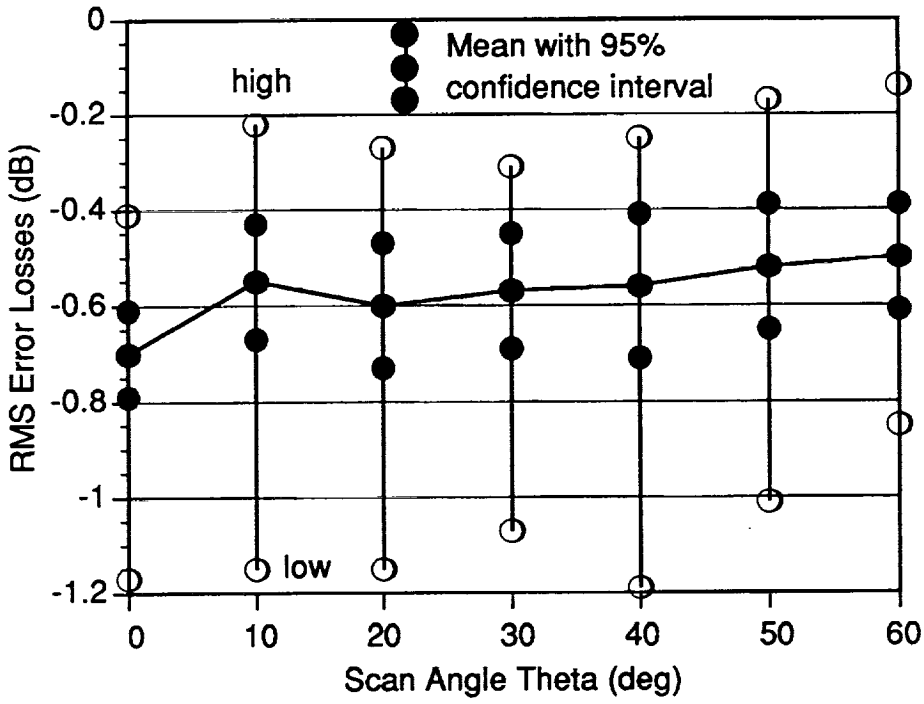

Figure 20. Random error loss for GE 8x2 array.

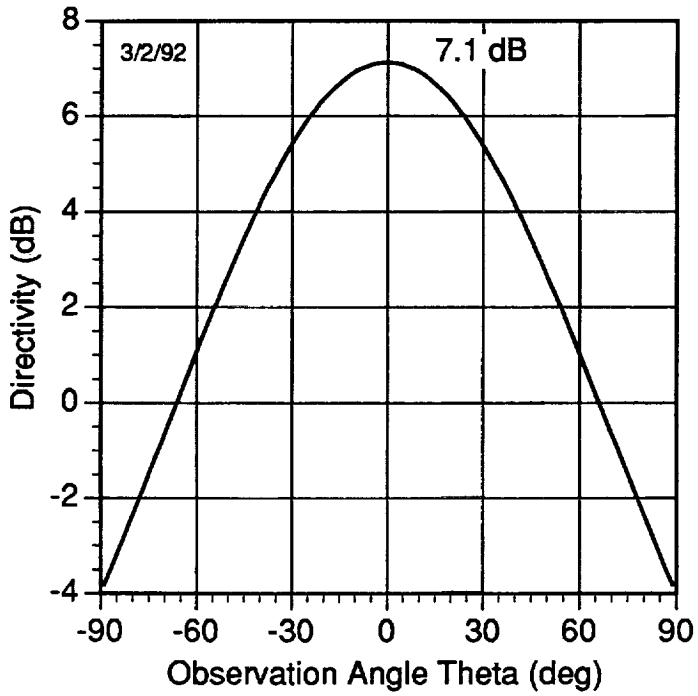

Figure 21. Element pattern for the Boeing array (phi = 0° plane).

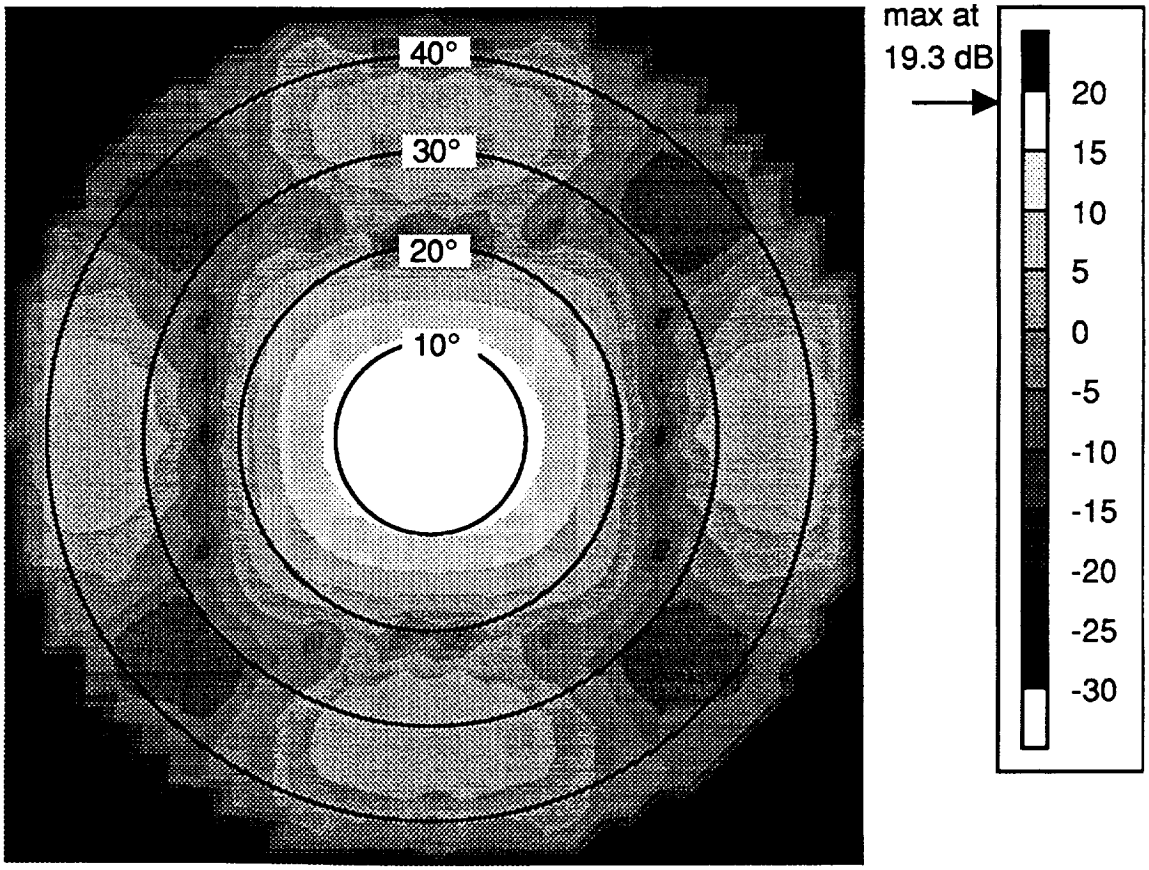

Figure 22. Contour plot for Boeing 23-element array shown for broadside scan for observations out to theta = 45°.

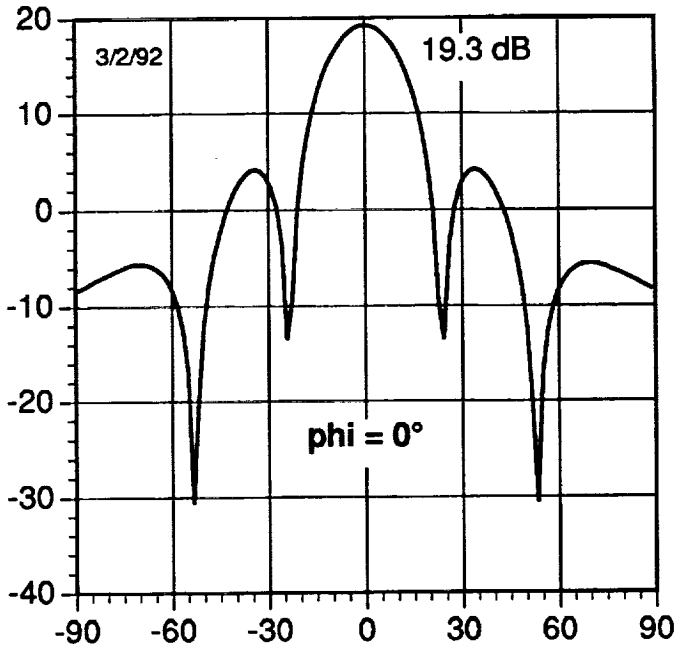

(a)

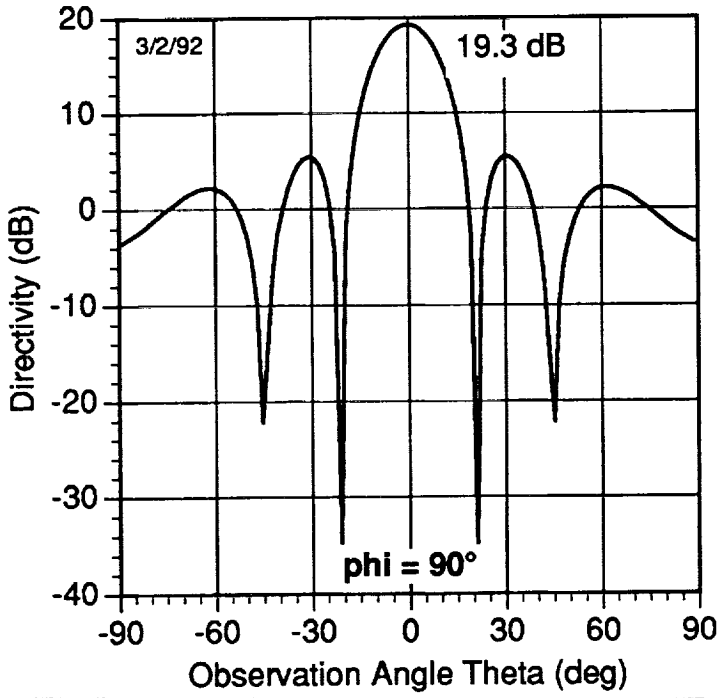

(b)

Figure 23. Boeing 23--element array far-field pattern at boresight for: (a) phi = 0° plane and (b) phi = 90° plane.

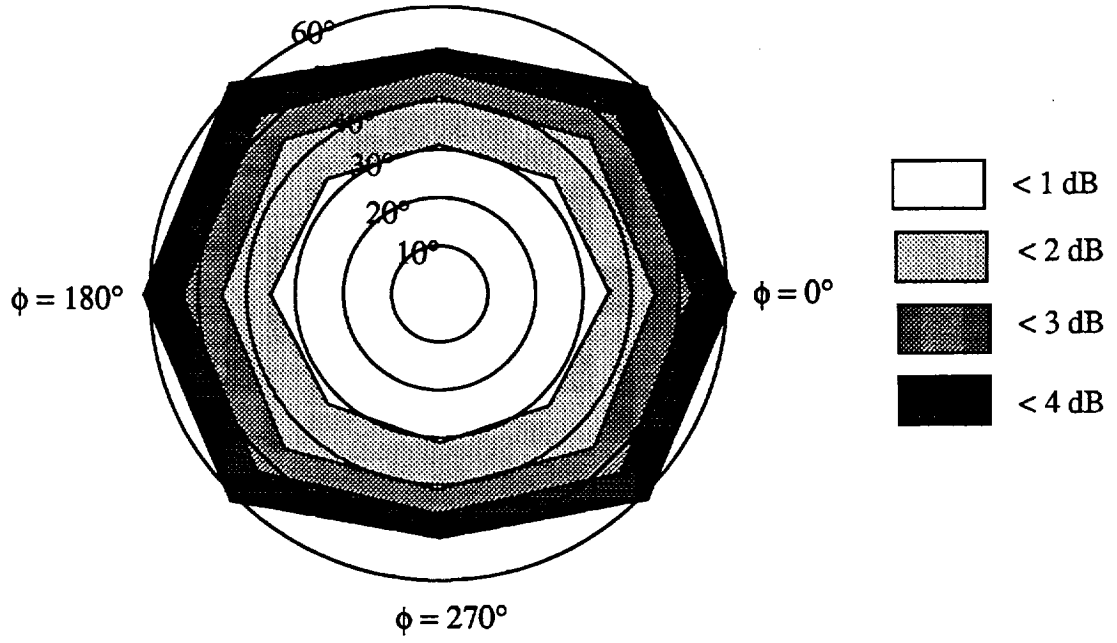

Figure 24. Scan loss for Boeing 23-element array.

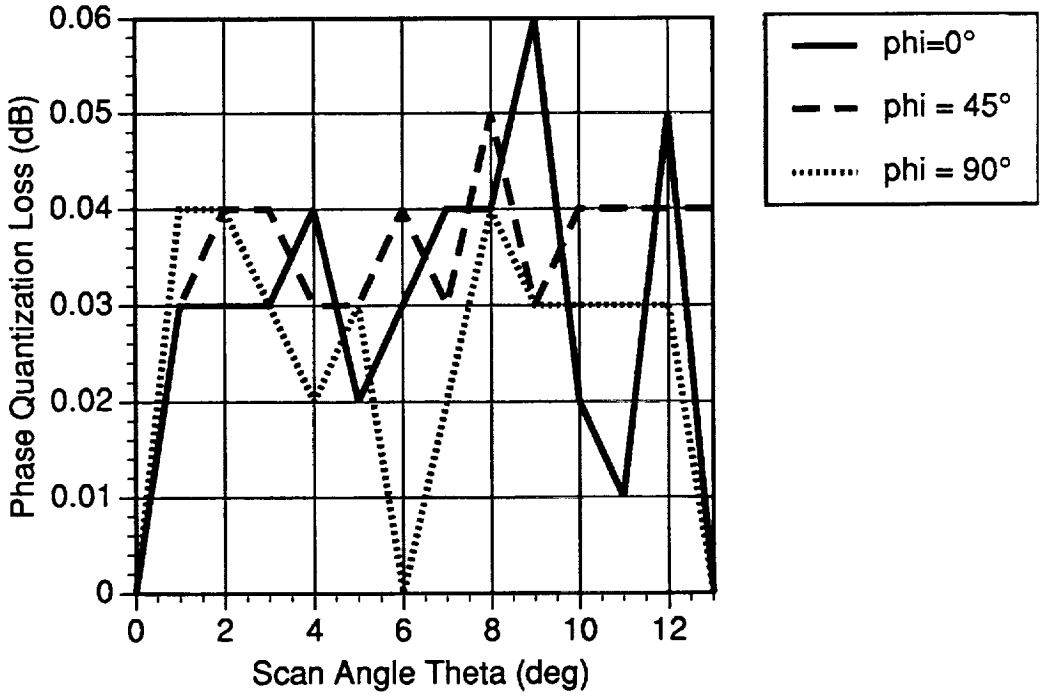

Figure 25. Phase quantization loss for the Boeing 23-element array.

REPORT DOCUMENTATION PAGE

Form Approved
OMB No. 0704-0188

1. AGENCY USE ONLY (Leave blank)	2. REPORT DATE	3. REPORT TYPE AND DATES COVERED
	March 1993	Technical Memorandum

4. TITLE AND SUBTITLE
Analysis of MMIC Arrays for Use in the Acts Aero Experiment

5. FUNDING NUMBERS
WU-506-72-1C

6. AUTHOR(S)
M. Zimmerman, R. Lee, E. Rho, and Z. Zaman

7. PERFORMING ORGANIZATION NAME(S) AND ADDRESS(ES)
National Aeronautics and Space Administration
Lewis Research Center
Cleveland, Ohio 44135-3191

8. PERFORMING ORGANIZATION REPORT NUMBER
E-7682

9. SPONSORING/MONITORING AGENCY NAMES(S) AND ADDRESS(ES)
National Aeronautics and Space Administration
Washington, D.C. 20546-0001

10. SPONSORING/MONITORING AGENCY REPORT NUMBER
NASA TM-106073

11. SUPPLEMENTARY NOTES
M. Zimmerman, Analex Corporation, 3001 Aerospace Parkway, Brook Park, Ohio 44142. R. Lee, E. Rho, and Z. Zaman, NASA Lewis Research Center. Responsible person, R. Lee, (216) 433-3489.

12a. DISTRIBUTION/AVAILABILITY STATEMENT
Unclassified - Unlimited
Subject Category 17

12b. DISTRIBUTION CODE

13. ABSTRACT *(Maximum 200 words)*

The Aero Experiment is designed to demonstrate communication from an aircraft to an Earth terminal via the ACTS. This paper describes the link budget and antenna requirements for a 4.8 kbps full-duplex voice link at Ka-Band frequencies. Three arrays, one transmit array developed by TI and two receive arrays developed by GE and Boeing, were analyzed. The predicted performance characteristics of these arrays are presented and discussed in the paper.

14. SUBJECT TERMS
MMIC arrays; Ka-Band; ACTS experiment

15. NUMBER OF PAGES
28

16. PRICE CODE
A03

17. SECURITY CLASSIFICATION OF REPORT	18. SECURITY CLASSIFICATION OF THIS PAGE	19. SECURITY CLASSIFICATION OF ABSTRACT	20. LIMITATION OF ABSTRACT
Unclassified	Unclassified	Unclassified	